

## PETROGRAPHIC AND MICROTTEXTURAL ANALYSES OF MIOCENE SANDSTONES OF ONSHORE WEST BARAM DELTA PROVINCE, SARAWAK BASIN: IMPLICATIONS FOR POROSITY AND RESERVOIR ROCK QUALITY

*Abdullah Musa Ali\*, Eswaran Padmanabhan and Hassan Baioumy*

*Department of Geosciences, Faculty of Geosciences and Petroleum Engineering, Universiti Teknologi PETRONAS (UTP), 31750, Tronoh, Perak, Malaysia*

Received February 9, 2016; Accepted May 6, 2016

---

### **Abstract**

The Miocene Miri Formation of West Baram delta is the most prolific formation of Onshore Sarawak Basin in terms of hydrocarbon accumulation. Despite their similarity in age and arenaceous composition, the prolific hydrocarbon occurrence in Miri Formation has not been reflected in the adjacent Belait and Lambir formations likely due to failure to identify discrete reservoir units in the formations. Thus, this study attempts to augment exploration in onshore West Baram Delta by analyzing petrographic and microtextural variations in Belait and Lambir formations using thin sections and Field emission scanning electron microscopy (FESEM) images. Organic content and anoxic condition of deposition, Iron and carbonate precipitation, tangential and floating rock fabric were shown to define the texture of the Lambir sandstones, while the Belait rocks are characterized by sutured and deformed quartz grains. The Belait conglomerates reveal euhedral quartz crystals characterized by mechanical weathering defects (fractures and striations), which are potential nucleation sites that promote the growth of quartz cement which subsequently limits compaction. Conversely, the chemical weathering features (etchings, pitting, solution pits and notches) in Lambir sandstones provide sites for pore growth, while the carbonate intraclasts, pyrite frambroids and iron oxides inhibits quartz cementation, but infill pore spaces. In all, the study showed that the Lambir are comparatively a more porous formation.

**Keywords:** Sarawak basin; West Baram Delta; Lambir and Belait formations; microtextures; Field emission scanning electron microscopy (FESEM).

---

### **1. Introduction**

Hydrocarbons have been found in almost all of the offshore provinces of Sarawak basin [1], with only three major discoveries made in the onshore West Baram province, i.e., the Miri Anticline in 1910; Asam Paya in 1989, and the recently discovered Adong Kecil West [2]. Production in the onshore West Baram province has declined due to the shutdown of Miri field after cumulative production of 80 million stock tank barrels (MMSTB) [1], while PETRONAS reports [2] a mere daily production of 440 barrels of crude oil in Adong Kecil West. Thus, the prolific occurrence of hydrocarbon in the Miri Formation has not been equally reflected in the adjacent Belait and Lambir formations of the onshore West Baram delta, despite their similarity in age (Miocene), and slightly diachronous transitional contact with the Setap Shale source rock [3]. This can be attributed to failure to identify discrete reservoir units and source intervals in Onshore West Baram Delta [5-7], notwithstanding the fact that several related geologic studies have evaluated the structural and tectonic evolution, depositional sequences, and geochemistry of the delta [8-14].

Therefore, this study attempts to augment exploration in onshore West Baram Delta by analyzing petrographic and microtextural variations in sub-stratigraphic outcrop units of Belait and Lambir formations. This is significant because studies of shallow sandstones have been

shown to provide important clues on shallow diagenesis, and the evolution pattern of early diagenetic minerals, which in turn can be used to decipher reservoir rock quality [15-17]. Hence, this study characterizes variations in texture, fabric and diagenetic features for both Belait and Lambir formations in line with changes in depositional environment from fluvial to shallow and deep marine, and from oxidizing to reducing conditions. The outcome of this study would provide relevant information for better understanding of the reservoir rock quality of the constituent formations of West Baram delta province.

## 2. Geologic setting

The Sarawak Basin of NW Borneo forms the southern margin of the Oligocene-Recent South China Sea basin and its tectonic evolution is closely linked to rifting and sea-floor spreading in the South China Sea marginal basin [18]. The Sarawak Basin is most generally thought to originate as a foreland basin formed after the collision of the Luconia Block with the West Borneo Basement during the Late Eocene [19]. Tan and Lamy [21] proposed that the tectonic evolution of Northwest Borneo in late Cretaceous via the rifting of South China Sea basin resulted in the formation of the Rajang Accretionary Prism [1]. The prism became uplifted and eroded, forming the major sediment source for the younger sequences deposited to the north and northwest Sarawak [20]. Thus, Sarawak basin is interpreted as a post-orogenic foreland basin that resulted from the closure and uplift of a Late Cretaceous- Eocene proto-South China Sea or Rajang Sea. The sedimentary rocks of the Sarawak basin are transported by the Baram River and tributaries, and are underlain by paleogene molasses sediments [19]. Rocks in the Miri zone represent the lower part of the Sarawak basin succession which extends offshore into the continental margin comprising of Nyalau, Setap, Tan-gap, Sibuti, Belait, Lambir, Miri and Tunku Formations, and range in age from Oligocene to Pliocene.

### 2.1. Study area and sampling

As previously mentioned, the Belait and Lambir formations were selected because of their time-stratigraphic similarity to the productive Miri Formation (Miocene). The Belait Formation consists of a sequence fluvial conglomerates and pebbly sandstones at the base interbedded with generally pebble-free medium to fine-grained sandstones and minor mudstones [3,19-20,22-24], passing upwards via a heterolithic muddy facies into a transgressive (deepening) sequence of nearshore and offshore shallow marine sandstone and mudstone dominated by hummocky cross-stratified sandstone intercalated with shale [20]. The Formation is exposed along the northeastern corner of Labuan between Kubong Bluff and Bethune Head, along with exposures along JIn. Tg. Kubong and JIn. Lubok Temiang, as well as on Bukit Kubong. The Lambir Formation (Middle - Late Miocene) mainly consists of fine to coarse-grained sandstone, shale with minor limestone and marl, intercalations of sandy clay with bioturbation and ophiomorpha, indurated clayey ironstone and pyritic nodules [25-26]. Outcrops of Lambir Formation are exposed in Tusan Beach area, along Miri - Bintulu coastline [26]. The Formation is characterized by cross-beddings of trough, hummocky, herringbone and tabular structures. The geological map depicting the Belait and Lambir formations, as well as their sample points B and L, respectively is shown in Fig. 1.

## 3. Methodology

Optical microscopy of thin sections of the samples was used to obtain mineralogical, petrographic and diagenetic details of both formations. Plane and cross polarized transmitted light optical photomicrographs with a spatial resolution of 2  $\mu\text{m}$  were taken of all thin sections using a LEICA DM 750P attached with a LEICA MC170 HD camera at Universiti Teknologi PETRONAS. Modal analysis was done using a JMicrovision 1.2.7 program, with 500 points counted for each image for classification and to measure porosity. Morphological characterization, textural analysis and mineral identification of the samples was performed using a high-resolution field emission scanning electron microscope (FESEM: Carl Zeiss Supra 55VP FESEM; operated at 5 to 20 kV) domiciled in Universiti Teknologi PETRONAS, which is attached with an energy-

dispersive X-ray spectrometry (EDX) system. The imaging was carried out under variable pressure (VP) ranging from 2Pa to 133Pa and probe current between 1pA and 10nA.

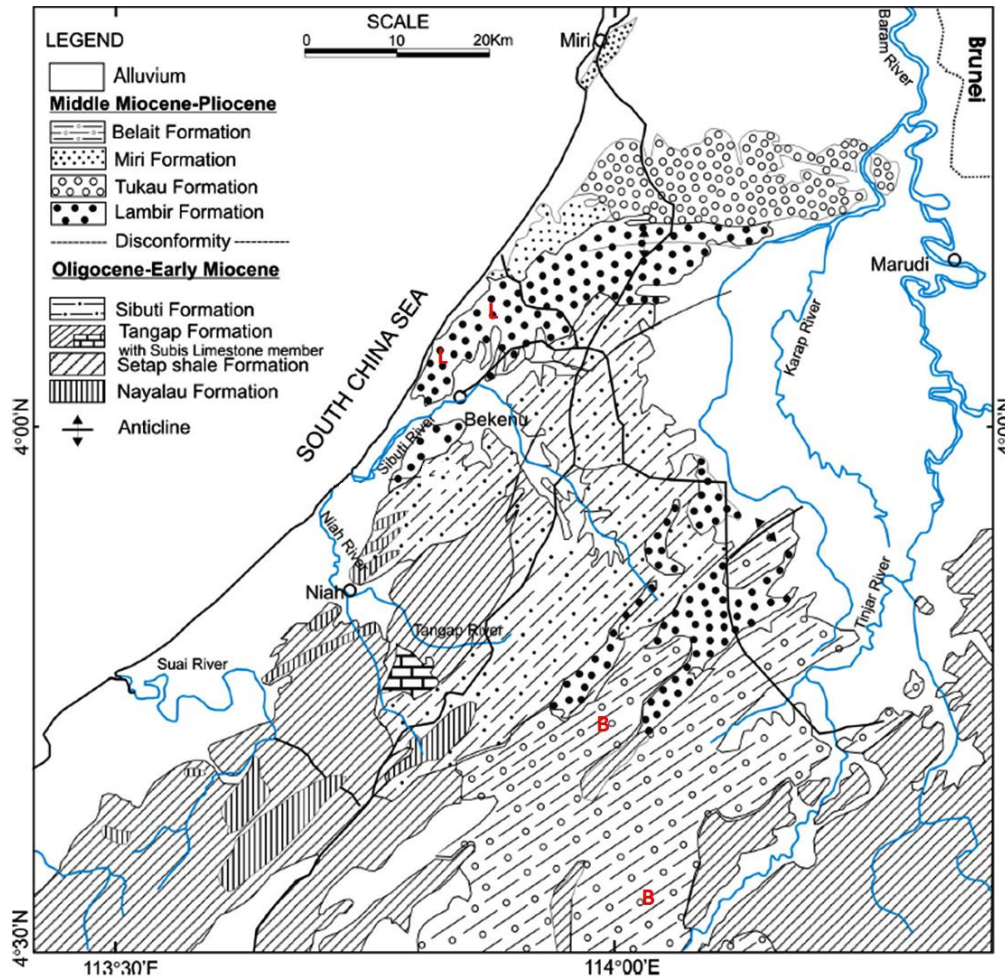


Fig. 1. Geology map of NW Borneo shows the study area (after Liechti *et al.* [3]; Nagarajan *et al.*, [27])

## 4. Results and interpretation

### 4.1. Thin section petrography

#### 4.1.1. Belait Formation

Belait formation consists of fluvial and shallow marine sandstone formations. The basal fluvial sandstones of the Belait Formation are polymict, given they comprise a differential range of gravel sized clasts (Indurated quartz sandstones) and coarse grained sandstones. The clasts consist of well consolidated/quartz-cemented quartz arenites (B1) and ferruginous well consolidated quartz arenites (B2). The shallow marine lithofacies analyzed comprise indurated ferruginous sandstone (B3) and Indurated clayey sandstone (B4).

##### 4.1.1.1. Fluvial sandstone lithofacies

###### **Well consolidated/quartz-cemented quartz arenites (B1)**

The well consolidated/quartz-cemented quartz arenites (B1) comprises predominantly detrital microcrystalline quartz grains, which are sub-angular to sub-round in shape, and medium to coarse sized with moderate sphericity and minor intergranular spaces (Fig. 2A). Most grains range from 0.2 to 0.5mm in diameter. The shape of the grain aggregates can be described as equigranular-polygonal (granoblastic) given the uniform distribution (well sorting)

of the subhedral grains (Fig. 2A). The grain boundaries of individual intraclasts appear to be both straight and sutured. The grain contacts also consist of quartz overgrowths abutting into original pore space (Fig. 2C). Some of the quartz intraclasts exhibit undulose extinction  $> 5^\circ$  while others display deformational twinning (lamellae) attributed to the extensive planar and conchoidal fractures, and imbrications/crenulations shown in the inset box of fig. A (Fig 2D). The interlocked and sutured grains are suggestive of concomitant compaction and cementation by dissolved silica and quartz overgrowth.

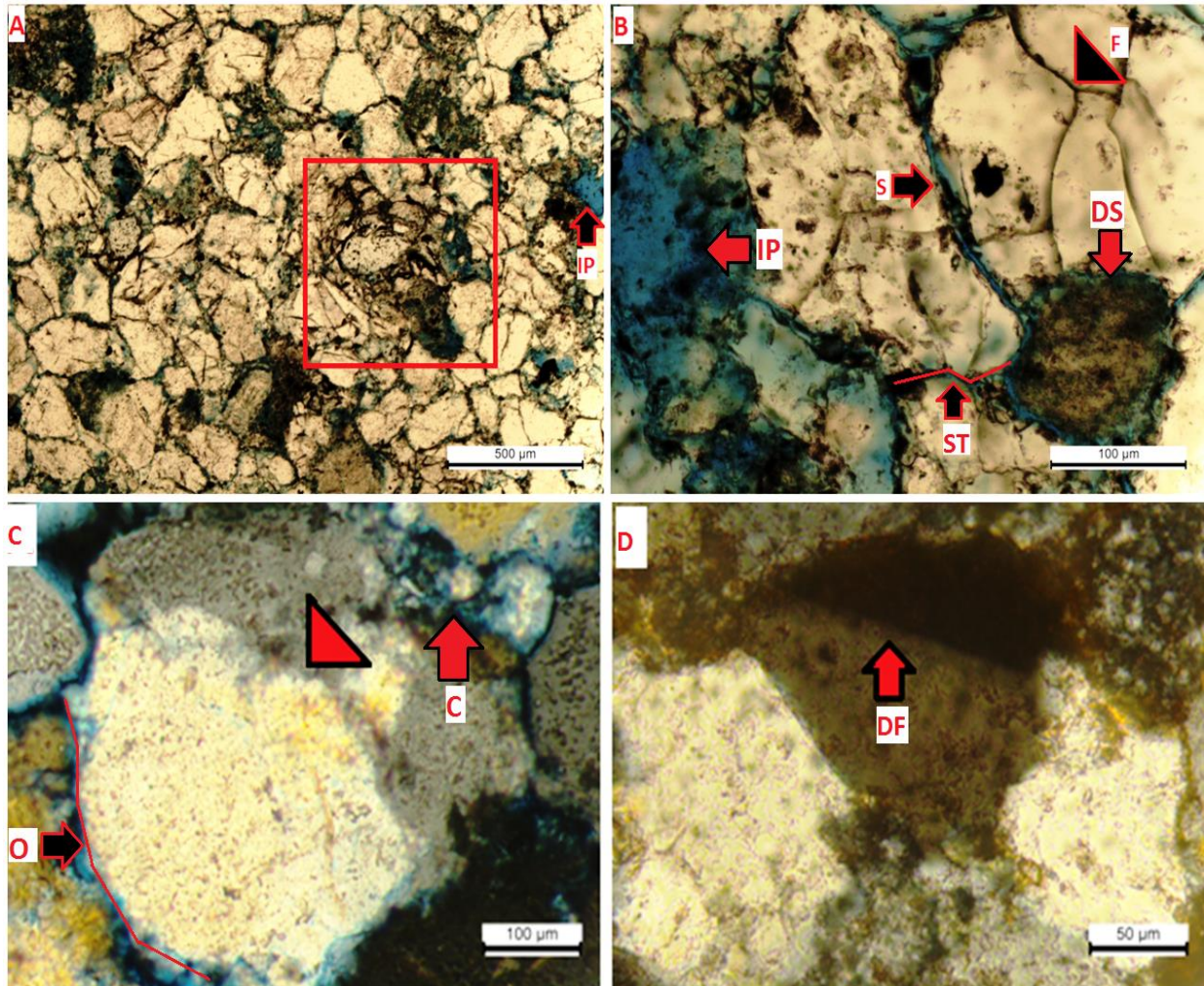


Fig.2. Thin section micrographs showing a] equigranular sized detrital quartz with inset box depicting imbrication of the grains, B] fractured grain (F) with intergranular pores (IP). The grain boundaries comprise of straight/line (S) and sutured (ST) C] disrupted undulose extinction, quartz overgrowth (O) and crenulations (C), D] deformational twinning

### **Ferruginous well consolidated quartz arenites (B2)**

The ferruginous well consolidated quartz arenites (B2) comprise of fine to medium grained sub-angular to sub-round detrital quartz intraclasts, weathered biotites (Fig. 3A), and plagioclase feldspar which is identified by its distinctive twinning (Fig. 3D). The iron oxide minerals present gives the rock its characteristic brownish color. The iron oxide coats the quartz grains and infills intergranular pore spaces as shown in Fig. 3B. The interlocking quartz intraclasts are characterized by sutured grain boundaries, and line and tangential (point) contacts that are not easily discernible under plane polarized light, but recognizably in cross-polarized light (Fig. 3B). The shape of the grain aggregates is defined as equigranular-polygonal

structure (granoblastic) (Fig. 3C). The fabric orientation shows platy (flaky) arrangement of the detrital quartz grains. Kaolinities are also identified interlocked with the detrital grains. The stability of the clast in terms of absence of mechanical features such as fractures and the presence of hydrous aluminosilicates (biotite) are attributable to durability (grain suturing and compaction) and proximal distance to source material.

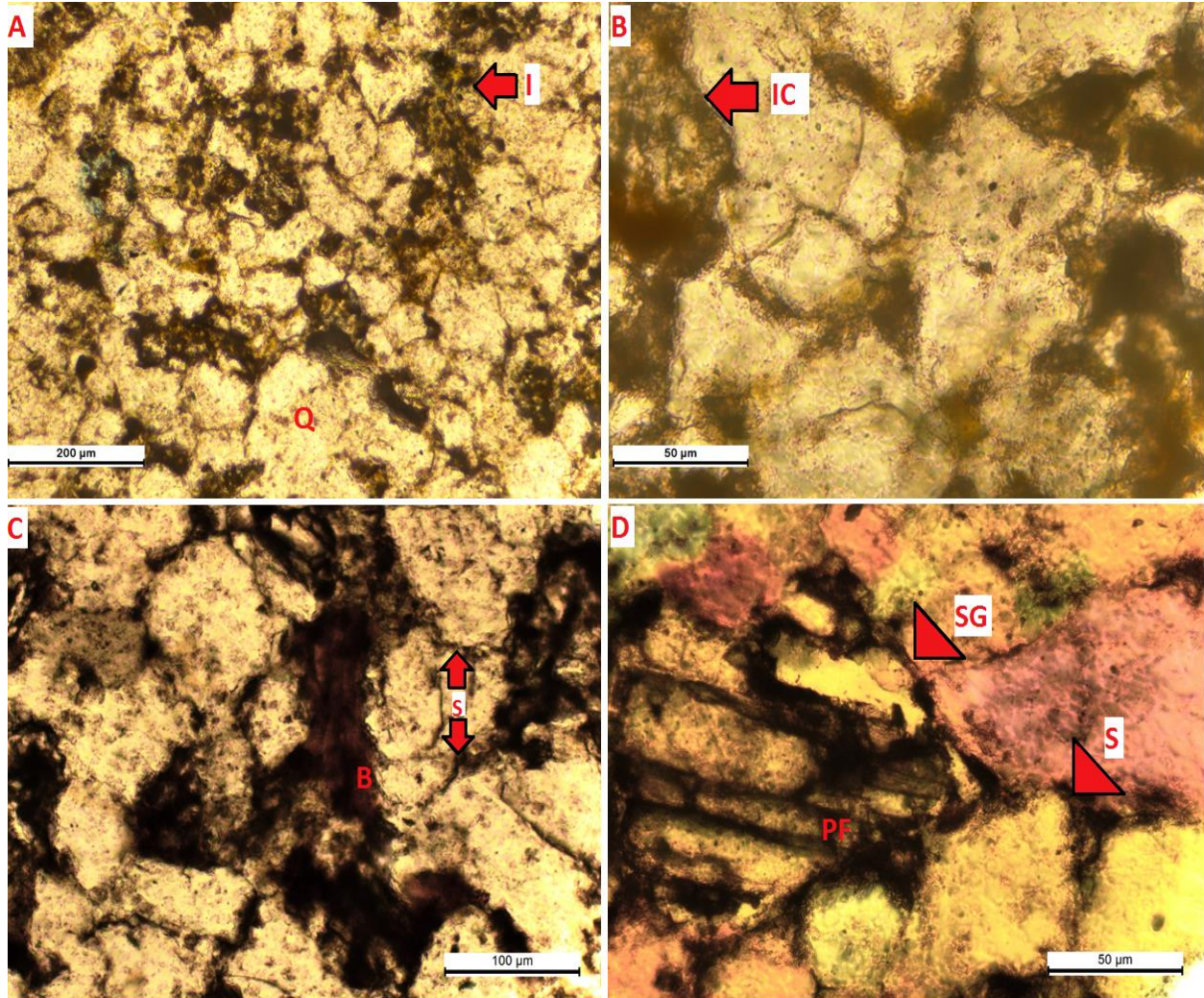


Figure 3. Optical micrographs of sample B1 from Belait Formation taken in plane-polarized light showing A] fractured and compacted quartz grains B] sutured grains with conchoidal fractures and pore infilling precipitated silica and calcium silicate (wollastonite), C] sutured quartz grains of optical continuity with weathered biotite (B), D] with plagioclase feldspar (PF) inclusions

#### 4.1.1.2 Shallow marine sandstone lithofacies

##### **Indurated ferruginous sandstone (B3)**

The facies comprises dominantly detrital fine grained monocrystalline quartz with minor occurrence of opaque mineral, possibly iron oxides, which partially infill intergranular pore spaces and coats the quartz grains (Fig. 4A). The sub-angular to sub-round quartz grains are characterized by moderate sphericity and moderately well sorted, with floating and poor point (tangential) grain packing with suturing in some areas (Fig. 4B). Although indurated, the sample is characterized by high intergranular pore spaces (Fig. 4B). The aggregates are characterized as equigranular-polygonal structure based on the well sorting of the subhedral quartz grains. The fabric of the detrital quartz grains shows randomly oriented platy/flaky

shape with minor occurrences of elongated grains, suggesting the reworking of sediments earlier deposited in quiet water by wave action (Fig. 4B). Also observed are planar and conchoidal fractures of the quartz surface indicating abrasion during sediment transport or compaction by overburden pressure, (Fig. 4A).

**Indurated clayey sandstone (B4)**

The detrital component of the Indurated clayey sandstone (B4) comprises predominantly of very fine sand sized monocrystalline quartz grains, clay, and iron oxides (Fig 4C). The moderately spherical quartz grains are moderately sorted, sub-angular to sub-round in shape and slightly fractured (Fig. 4C). The boundaries of the grains are delineated by a thin iron oxide – clay coating between the overgrowth and the grain (“dust-line”) observed in Fig. 4D. The grain packing consists of floating and point (tangential) grain contacts, with intergranular pore spaces filled by clay minerals. The particle orientation can be described as randomly oriented flaky/platy grains.

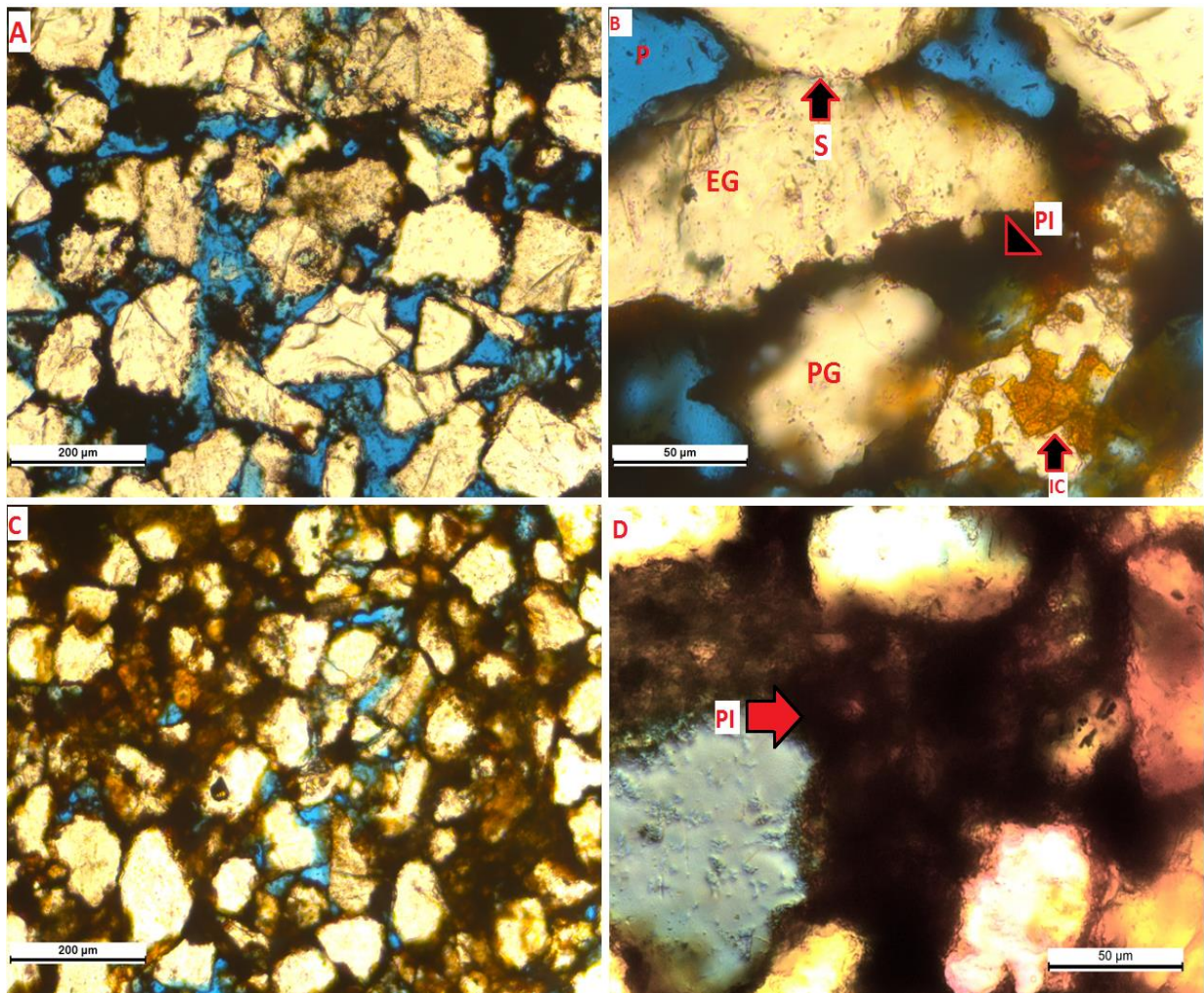


Figure 4. Optical micrographs of A] detrital monocrystalline quartz grains, clay and carbonate matrix B] mixture of elongated (EG) and platy (PG) quartz grains thin iron oxide – clay coating between the overgrowth and the grain (a “dust-line”) C] high intergranular porosity and partial infilling of pore spaces between fractured detrital quartz grains D] iron oxide coating of the quartz grains and infilling of intergranular spaces

#### 4.1.2. Lambir Formation

The shallow marine sandstone lithofacies of Lambir Formations show petrographic variations and are categorized into sub-facies: friable ferruginous granular sandstone (L1); Indurated laminated ferruginous sandstone (L2); Pyritic sandstones (L3), and calcareous sandstones (L4).

##### 4.1.2.1. Shallow marine sandstone lithofacies

###### **Friable ferruginous granular sandstone (L1)**

The sample comprises predominantly of fine sand-sized detrital quartz grains, with opaque (iron bearing) minerals and rock fragments as shown in Fig. 5A. It is highly porous and uncompact with moderately sorted and slightly coated grains. The grains are sub-angular in size with floating and point (tangential) grain contacts as shown in the micrograph in Fig 5A&B. The grains are slightly fractured and exhibit moderate sphericity as depicted in Fig. 5A. The particle orientation of the rock can be described as randomly distributed platy / flaky and minor elongated grains. Evident is the low amount of clay matrix and cement material. The friability of the sample indicates post-depositional surficial hydration and leaching. The iron oxides possibly results from heavy-mineral placement formed by mechanical concentration of high specific gravity minerals, largely associated with beach/marine sediments (Boggs, 2009). The grain texture suggests far distance from source and mechanical weathering via wave or tidal action in shallow marine environment.

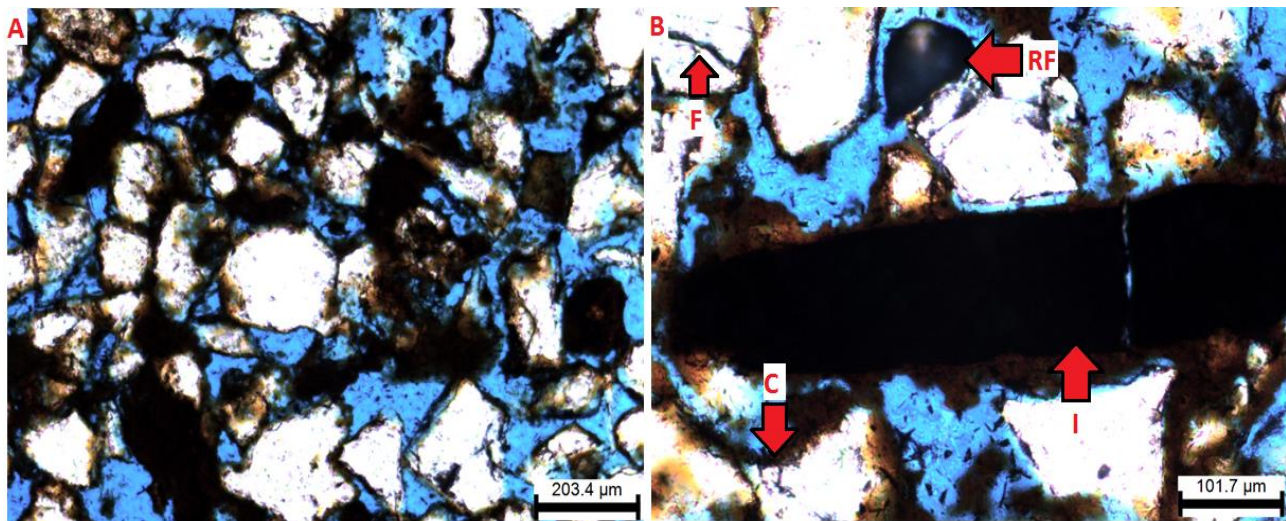


Fig 5. Optical micrographs of sample L3 showing A)] very fine to fine sand sized, slightly fractured quartz grains with high intergranular pores, and iron oxide inclusions (I), B)] rock fragments (RF), grain coating (C), fractures (F)

###### **Indurated laminated ferruginous sandstone (L2)**

The framework detrital component consists of predominantly fine sand sized quartz grains. Minor occurrences of larger quartz grains, iron oxides and organic matter forming the matrix materials are also identified (Fig. 6A). The concentrated presence of iron oxides and organic matter is clearly evident from the deep black color of the rock. The moderately well sorted quartz grains vary from sub-angular to sub-rounded, and of high sphericity. The shape of the grain aggregates can be described as inequigranular polygonal structure given the disparate particle distribution. The grain packing of this rock type is characterized by floating and point (tangential) grain contacts with line and concavo-convex contacts in some areas, due to low compaction resulting in high porosity. Grain coating are also observed, with clay materials infilling and lining intergranular pores. Few fractures are observed, although dissolution pit is seen. The packing orientation suggests preferred alignment of both platy and elongate grains.

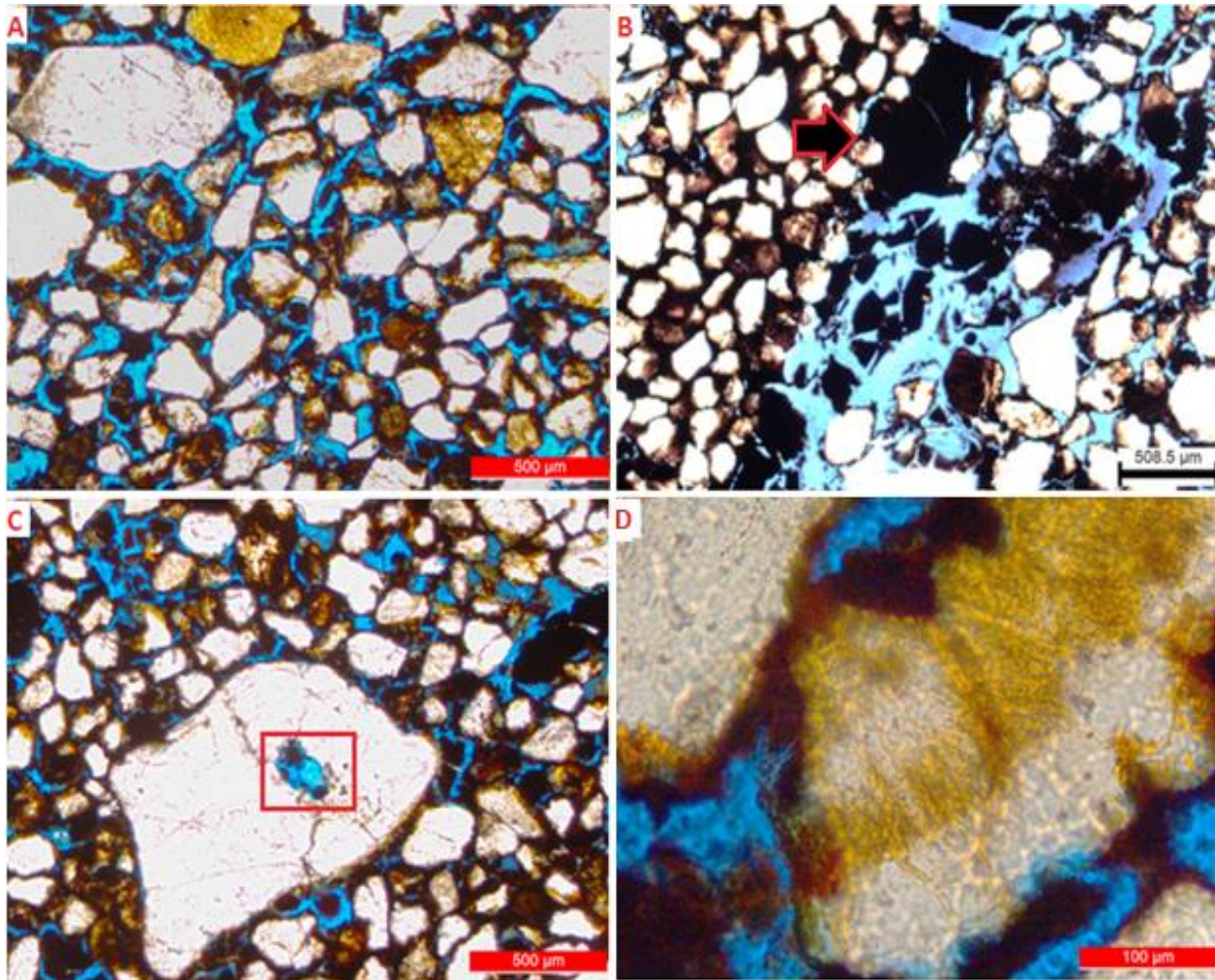


Fig 6. Optical micrographs of sample L1 showing A] fine sand sized quartz grains with minor occurrences of coarse grains, B] re-organization of the grains in alignment with organic matter, c] Quartz surface fracture, dissolution, D] pore infilling grain coating by organic matter and iron oxides staining and coating of the quartz grains.

### ***Pyritic sandstones (L3)***

This porous lithofacies consists of friable ferruginous sandstone, pyrite with organic matter and rock fragments (Fig. 7A). The highly fractured quartz grains vary from fine grained to coarse grained sediments. The grains are sub-rounded with high sphericity and moderately sorted indicating textural sub-maturity. Opaque minerals like iron oxides and rock fragments are also observed. Similarly, the sample is characterized by point (tangential) grain contacts (Fig. 7B). Distinctive for this rock type is high Intergranular porosity due to possibly leached matrix content during weathering, burrows and lack of quartz cementation (Fig. 7C). The organic matter also plays a large role by preserving the porosity, widening existing pore spaces and engulfing the quartz grains (Fig. 7D). The detrital quartz grains are observed to be preferentially aligned along the axis of the organic matter particles (Fig. 7B). The authigenic fine-grained clay-rich matrix material formed from the mechanical and chemical degradation of primary framework grains such as feldspar, as well as through mechanically infiltration into the Intergranular pore spaces. The matrix also shows high enrichment of organic matter, sulfates and increased friability, all indicating reducing anoxic conditions.

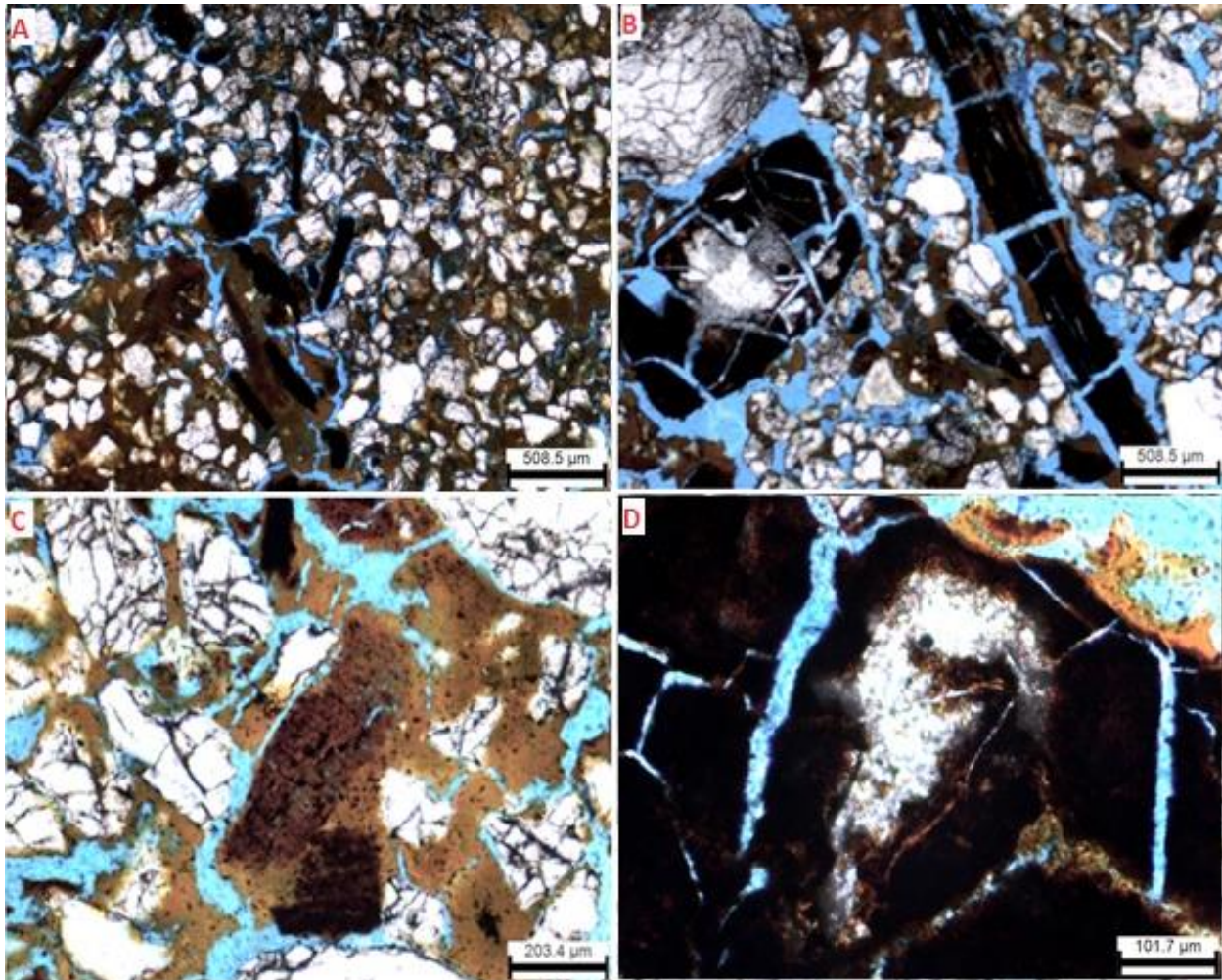


Fig 7. Optical micrographs of sample L2 showing A] highly fractured quartz grains, clay matrix, organic matter, and rock fragments, B] re-alignment of the quartz grains along the axis of the columnar shaped organics C] organic matter remnant enclosed in the clay matrix D] clay material infilling of intergranular pore spaces E] desiccated clay material occupying pore spaces F] closer view showing quartz grain embed in organic matter

#### ***Indurated calcareous sandstones (L4)***

The detrital components comprise monocrystalline fine grained quartz enclosed in crystallized calcite cement (Fig. 8A). The detrital quartz grains are very fine to fine sand size, sub-rounded to sub-angular, with moderate sphericity (Fig. 8B). The quartz grain packing shows floating and point (tangential) kinds of grain contacts. The random arrangement of the platy quartz grains encased in calcite cement (Fig. 8A) can be referred to as inequigranular-polygonal. Opaque minerals (possibly iron oxides) are also observed in Fig. 8B. The compactness of the rock is indicated by the absence of intergranular porosity. The quartz grains show incipient rounding, evident of the reworking process, while grain angularity partially results from the attaching and partial replacement of quartz grains by calcareous cements.

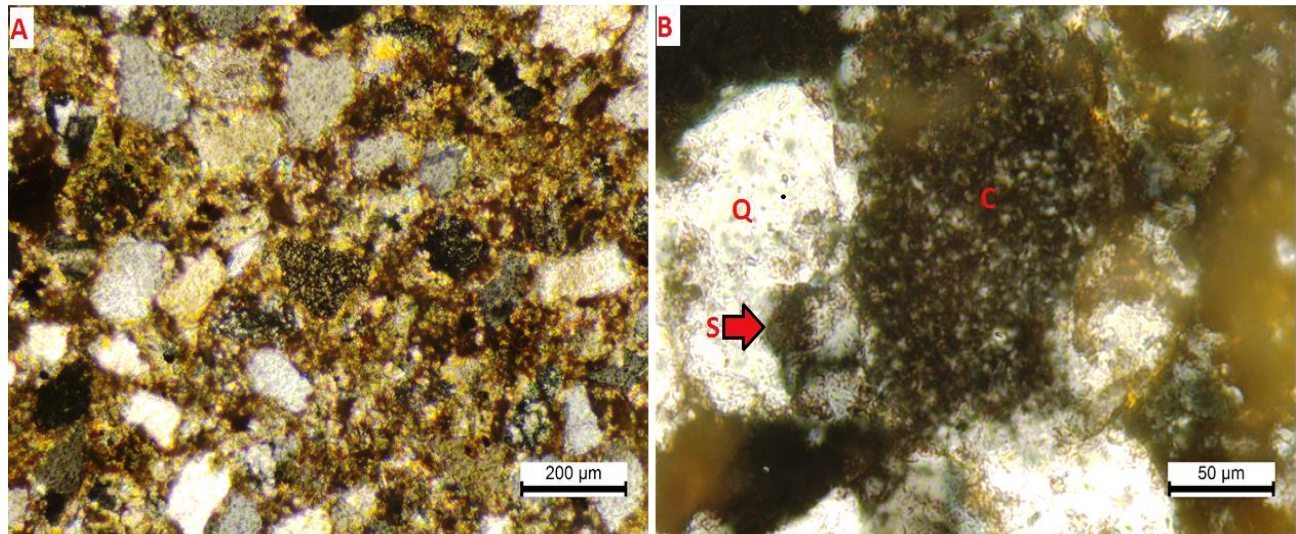


Fig 8. showing A] fine grained quartz that have been well cemented with calcareous matrix B] floating and point (tangential) kinds of grain contact with random arrangement of the elongated grains indicating quiet water deposition

## 4.2. Scanning electron microscopy (SEM) analysis

### 4.2.1. *Belait Formation*

The ubiquitous features in the samples are those related to weathering and diagenesis, which include weathered surfaces, mechanical weathering features, dissolution etching, and silica precipitation, which occur in high abundances in most of the samples. Some samples consist of quartz coated with authigenic iron oxides, clay materials and organics cement, where the quartz grain is hardly visible as a result of crystallographic degradation.

#### 4.2.1.1 *Fluviatile conglomerate lithofacies*

The surfaces of the Belait Indurated quartz sandstones (B1) depicted in Figs 9 (A&B) reveal euhedral angular and sub-angular quartz crystals with well-defined faces and polygonal texture. Identifiable structural features and micro relief markings include conchoidal fractures (CF), serrated edges (SE), striations (S) and granulations (G), flat cleavage planes (CP), imbricated grinding features, and irregular ridges (IR). The conchoidal fracture is identified by its curved irregular depression which is stepped in a sequence of ridges.

Similarly, the quartz grain surface of the ferruginous siliciclastic conglomerate clast (B2) consists predominantly of conchoidal fractures (CF) or breakage patterns, which vary in shape and sizes, and are irregularly distributed. Clearly discernible is the convex elevations of the conchoidal fracture (Fig. 9C). Straight and arcuate steps closely associated with conchoidal fractures are also present. The observed chlorites ranges from clusters of elongate to disc-like authigenic crystals pressed to the quartz surface or partly filling a depression within detrital quartz grain (Fig. 9D). The notches of ferruginized sandstone conglomerate are sparsely distributed on the quartz grains from and are generally uniform in size and shape. The smooth undulating quartz surface, angular quartz face, distinctively sharp crystal edges and minute size of the notches indicate absence of chemical dissolution.

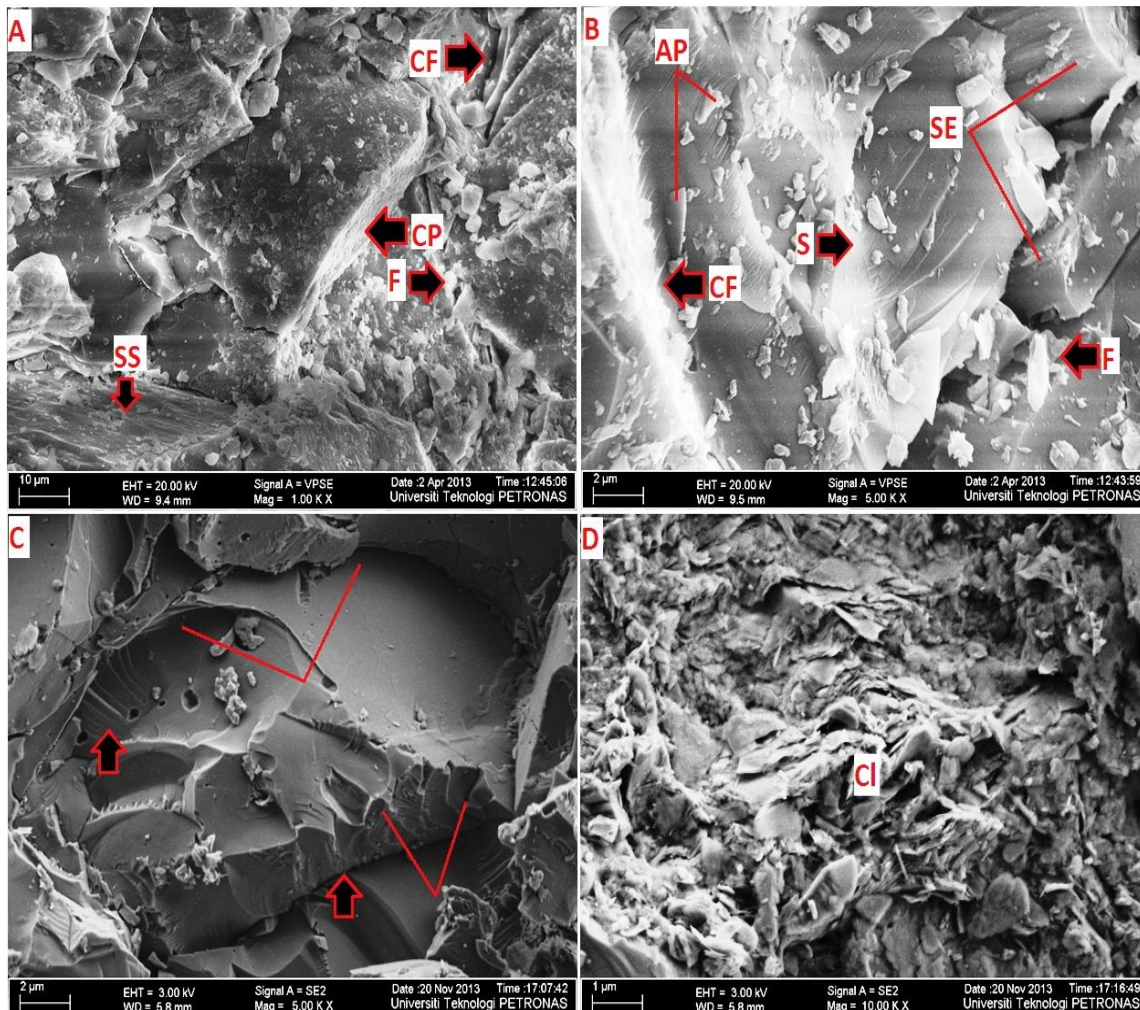


Fig 9. Sample B1 showing (A) crystalline quartz grains with distinct polygonal texture showing normal (F) and conchoidal fracture (CF), cleavage planes (CP) and striations (S); (B) Closer look of crystalline quartz grains at 1000x magnification showing striation marks (S), serrated edges (SE), adhering particles (AP) normal fracture (F) C] Sample B2 showing conchoidal fracture (CF) with straight (SS) and arcuate steps (AS) and linear fracture (F) and D]chlorite minerals

#### 4.2.1.2 Shallow marine sandstone lithofacies

##### **Indurated ferruginous sandstone (B3)**

The general outline of the B3 shows quartz extensively coated with iron oxides and poorly crystallized flakes of authigenic clay minerals making the quartz grain almost indiscernible, although the sub-rounded to sub-angular form is observable (Fig. 10A). The clay minerals infill (PI) and bridge the intergranular spaces, denoting grain-supported fabric (Fig. 10B). Identifiable features of the quartz surface include adhering particles (AP), v-shaped breakage patterns (VP), serrated edges (SE), notches (N), and irregular fractures (IR) all indicating the combined impact of mechanical and chemical weathering. The quartz surface appears to be scaling, disintegrating and generally flaking off (Fig. 10D), indicating intensive deterioration due to dissolution.

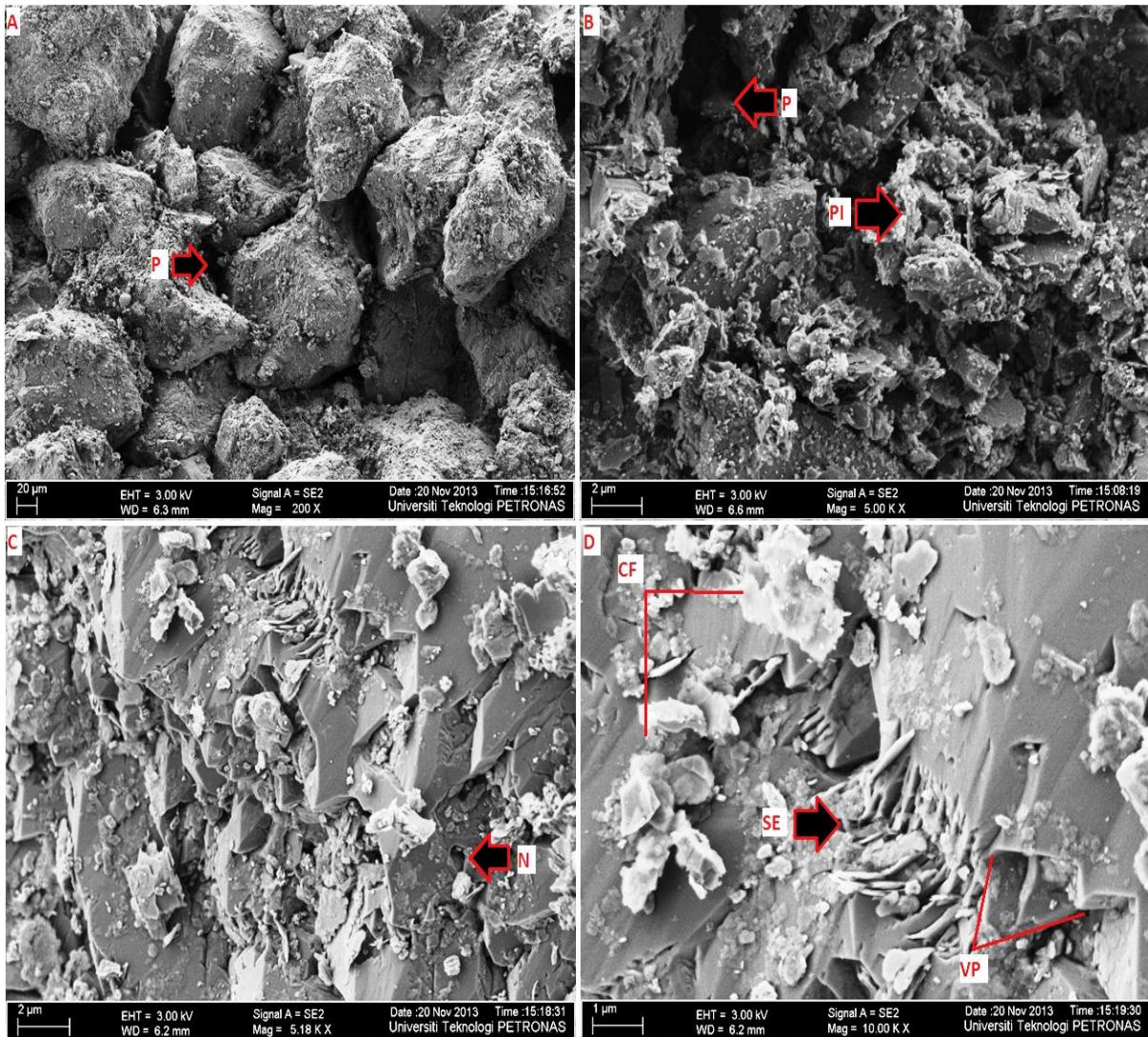


Fig.10. SEM micrograph showing iron (Fe) and clay flakes (C) adhering to quartz surface A) notches (N), striations (S) and silica precipitates (SP), irregular fractures (IR), adhering particles (AP), v-shaped patterns (VP) and serrated edges (SE) and B) sub-rounded quartz grains coated and bridged by clay minerals

### **Indurated clayey sandstone (B4)**

The B4 sample consists of angular subhedral quartz grains and clay minerals. The observed micro features on the quartz surface include conchoidal fractures (CF), cleavage planes (CP), dendritic etchings (DE) developed from adjacent conchoidal fractures, as well as surface etchings (SE) and straight striations (SS) (Fig. 11A), which are of mechanical or mechanical/chemical origin. The Intergranular space between the quartz grains is infilled with clay mineral as shown in Fig. 11B. Clay mineral crystals (illite and kaolinite) have aggregated in the pore throats of the sandstone and on the faces of the quartz grains. The illites are composed of irregular, flake-like clay platelets oriented parallel to each other are observed in Fig. 11C, which suggest illitization of kaolinite. The kaolinite occurs as face-to-face stacks of pseudo-hexagonal plates or books. The stacks of kaolinite appear to partially fill a pore (Fig. 11D).

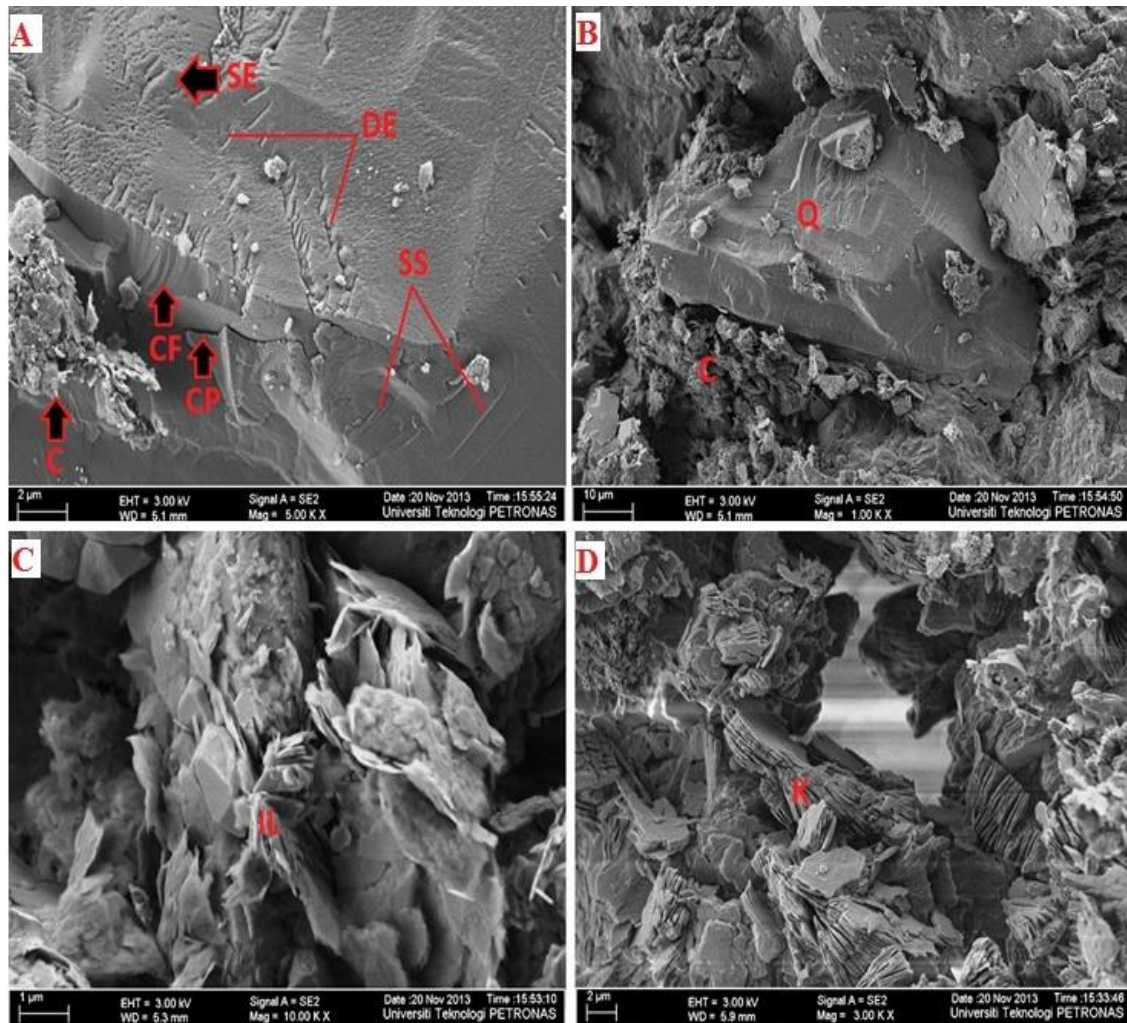


Fig.11. SEM micrograph of the quartz surface showing A] surface etchings (SE), conchoidal fractures (CF), dentritic etchings (DE), straight steps (SS), straight striations (SS) and cleavage plane (CP) notches (N), striations (S) and silica precipitates (SP), B] pore filling reducing porosity by clay minerals C] Massive detrital illite, D]kaolinite infilling pore spaces

#### 4.2.2. Lambir Sandstones

##### 4.2.2.1. Shallow marine sandstone lithofacies

##### **Friable ferruginous sandstones (L1)**

The quartz grains of are highly coated (Fig. 12A). The removal of the ferruginous coating reveals etched quartz surface (Fig. 12B). Features identified include etch pits, notches, parallel striations and chatter mark trails. A closer view shows markedly etched quartz surface, with some pits developing into notches (Fig. 12C). The mostly circular and sub-circular etch pits and notches are formed by grain-to-grain collision or mechanical breakdown due to wave action during fluvial transportation [28]. The observed straight striations (Fig. 12D) are attributable to high-energy transport in fluvial and/or littoral environments [29-30]. The sequence of linearly arranged, crescent-shaped grooves (crevasses on a grain surface) is referred to as chatter mark trails (Fig. 12D), resulting from friction via mechanical collision between sand grains that have been subjected to severe shocks related to intertidal beach environment, possibly in a wet tropical climate [31-32,43]. The association of different micro-textures in a single grain suggests that the sediments comprise grains derived from different sources.

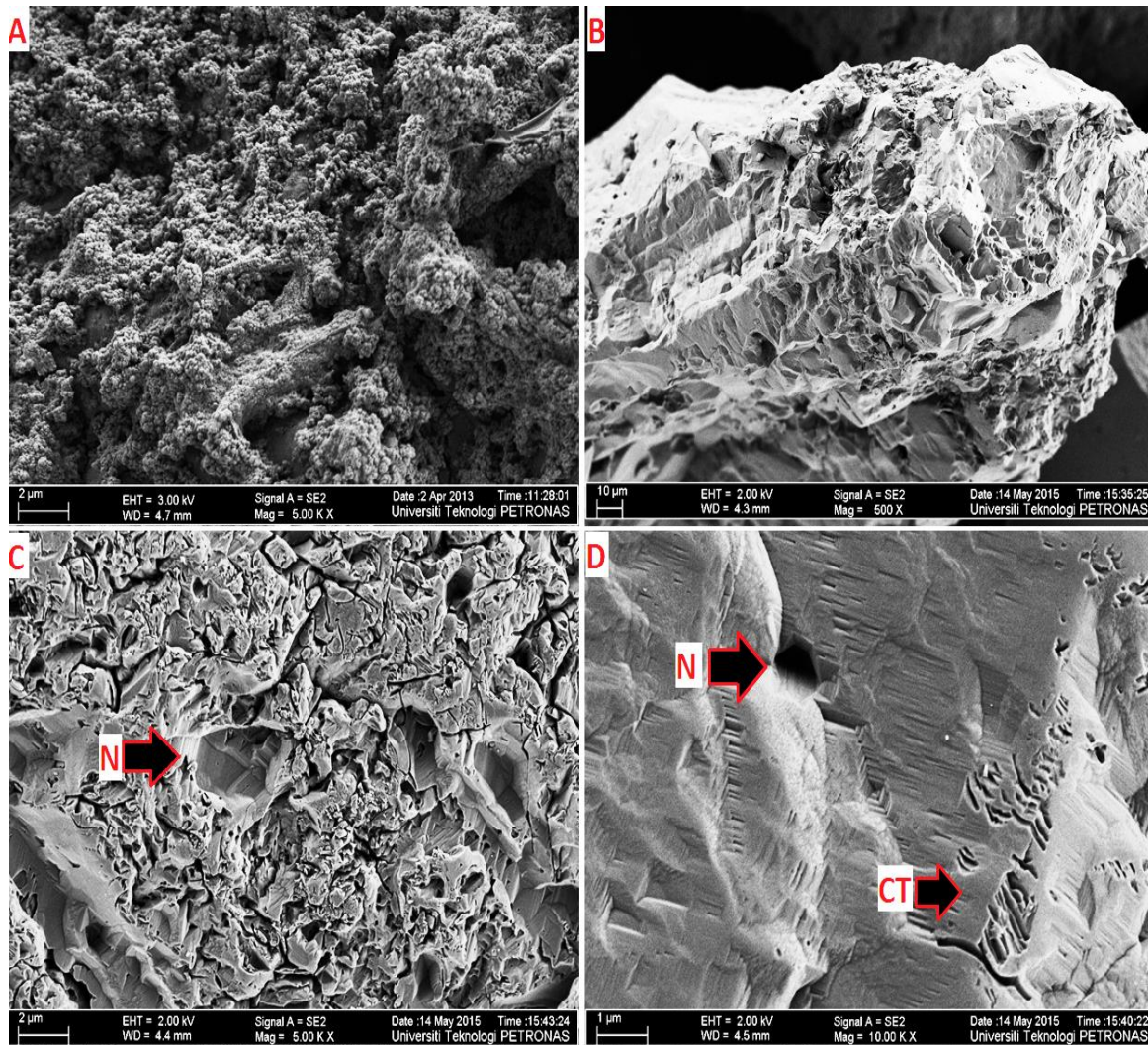


Fig.12. SEM micrograph of the quartz surface showing A] extensively coated grain surface, B] surface etchings of subangular quartz grain, C] deep etch pits and notches, D] notches (N), parallel striations and chattermark trails (CT)

### ***Indurated laminated ferruginous sandstone (L2)***

The representative sample consists of quartz coated with iron oxides and clay materials. The sub-rounded quartz grains are characterized by intergranular porosity (Fig. 13A). The quartz crystal is hardly visible as a result of crystallographic degradation by iron oxide coating as observed in Fig. 13B. Fractures and striations are observed on the clean quartz surface. The chatter mark trails present are mechanical/chemical features identified by their distinctive convex indentation or trail marks. The chatter marks (Fig. 13D) are randomly distributed across the quartz grain surface. Depending on the mode of origin, the chemical features are formed as a result of chemical dissolution and precipitation. Chemical features identified on the incompletely quartz surface include notches (N) and etchings (SE). The exposed surface morphology of this sample also comprises notches (N), solution pits (SP), silica precipitates that form adhered particles (AP), straight striations (SS) and grooves (G) (Fig. 13A). Figure B gives a closer view of the imbricate groove/gouge infilled by clay minerals. The gouge is a resultant feature of continual dissolution, expanding from solution pit to repositories for the accumulation of weathered minerals. The globular shaped silica precipitates also occur randomly in close proximity to the solution pits. The edges of the solution pits are lined with

precipitated silica (Fig. 13B). The notches formed by the chemical dissolution on quartz surface are in the form of micro circular pits (Fig. 13C).

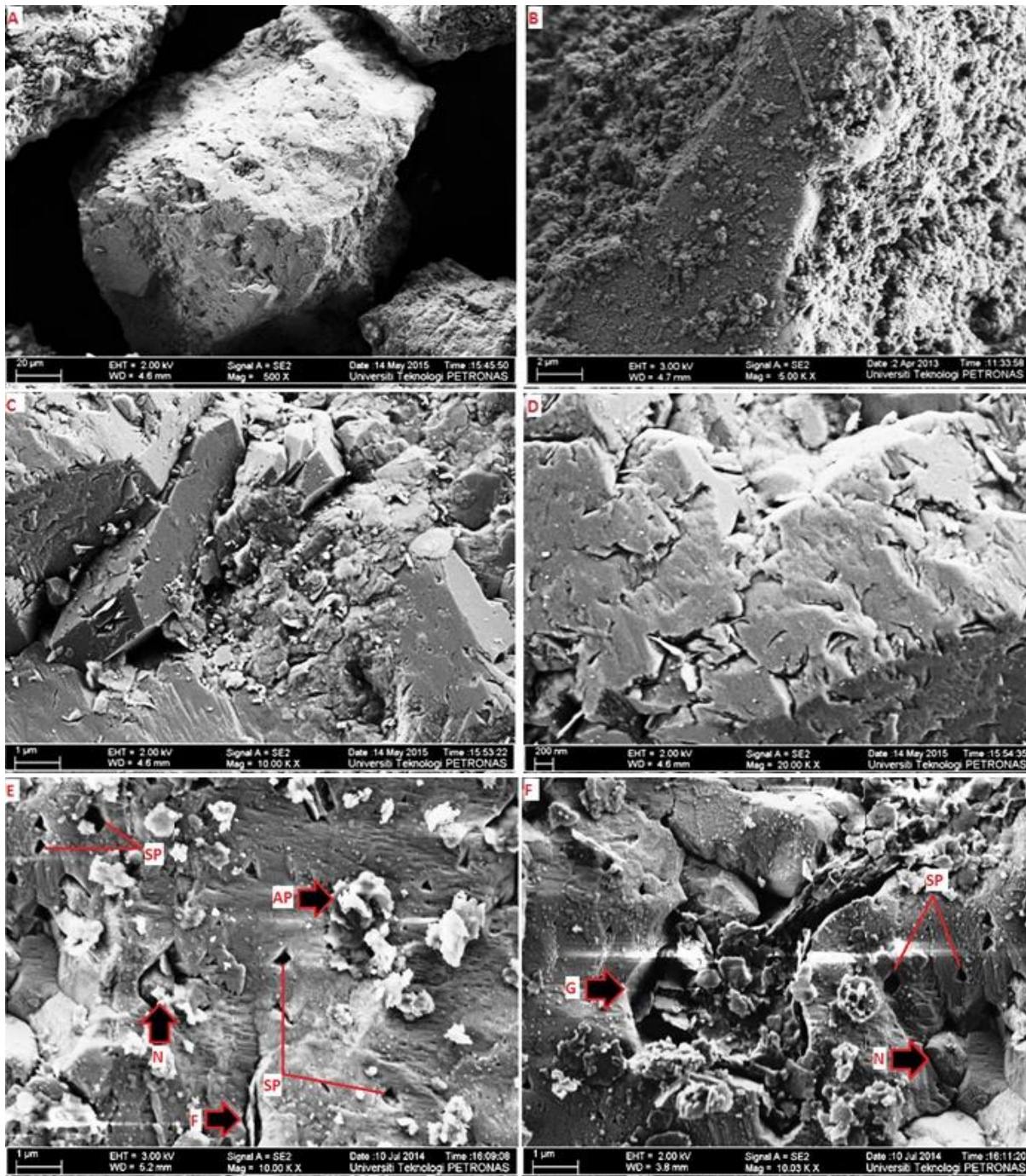


Fig 13. Iron oxide coating (IC), notches (NN), surface etchings (SE) and carbonate mineral (C), B) closer view of iron oxide coating of quartz surface, (A) Quartz grains coated with iron oxide and (B) closer view of iron oxide coating of quartz surface; solution pits (SP) C] notches (N), parallel striations (Pst), fractures (F), solution pits (SP) and adhering particles (AP) D] infilling of gouges (G) and solution pits (SP)

### **Pyritic sandstones (L3)**

Fig 14A of the L3 sample depicts frambroids of iron bearing (pyrite) minerals coating the quartz, and also infilling intergranular space. The pyrite and carbonate minerals (C) coat and bridge the pore between quartz grains. The extensive coatings are indicators of shallow marine environments (shelf and littoral), and other coastal environments (estuaries, deltas, lagoons). The pyrite frambroids are widely associated with bacteria sulfate reduction in marine sedimentary environment. The abundance of sub-rounded and angular grains with conchoidal fractures indicates its nearby provenance or proximity to source area. The rounded edge grain consisting of diverse microtextures such as v-shaped mechanical marks, straight striations, and adhering particles on its surface indicate that it was exposed to different provenance histories and multicyclic character. Chemical dissolution etching is an indicator of highly concentrated alkaline sea water or high dissolved amount of alkali metals in meteoric water.

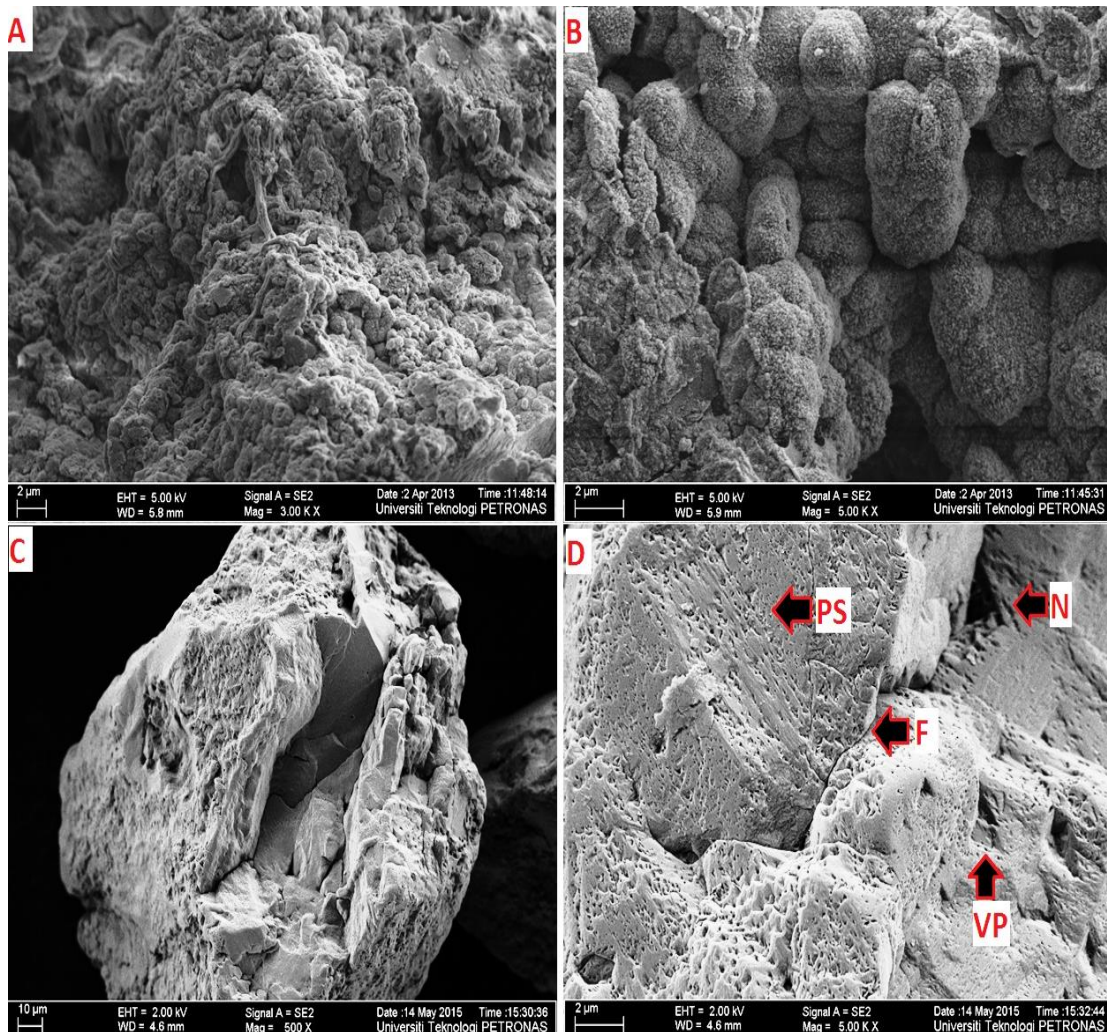


Fig. 14. The SEM micrographs showing A) pyrite frambroids quartz surface, B] Pyrite and carbonate mineral (C) coating and pore bridging of the quartz grains, C] quartz surface indentation D] etched and pitted surfaces, gouges/grooves, striations and fractures

### **Indurated calcareous sandstones (L4)**

The micrographs (Fig. 15A) of the Indurated calcareous sandstones (L5) shows detrital quartz grains (Q) coated with very fine-grained sucrosic, pore-lining and pore-filling calcite carbonate cement (Cab) and adjacent authigenic chlorite (C). The carbonate cement material (Fig. 15B) consists of clusters of small (2 to 5 $\mu$ m) rhombic calcite crystals. The chlorite

minerals occur as clusters of disc-like, authigenic crystals. The euhedral, pseudo-hexagonal crystals of chlorite are approximately less than 1µm thick. Other observable surface features include notches, which develop into solution pits, angular and straight striations (SS), and conchoidal fractures (CF) as shown in Fig. 15C. Silica flakes are also identified plastered on the surface, which are possibly products of dissolution from grain to grain impact or chemical etching. The notches present along the axes of striation (Fig. 15D) indicate a relationship between weakened planes and dissolution. Thus the striations provide a route for quartz dissolution. The shape of the subhedral grains signifies moderate distance of transport from source. However, the breakages, fractures, and microchips resulting from imbrications suggest rapid sedimentation and tumultuous depositional environment.

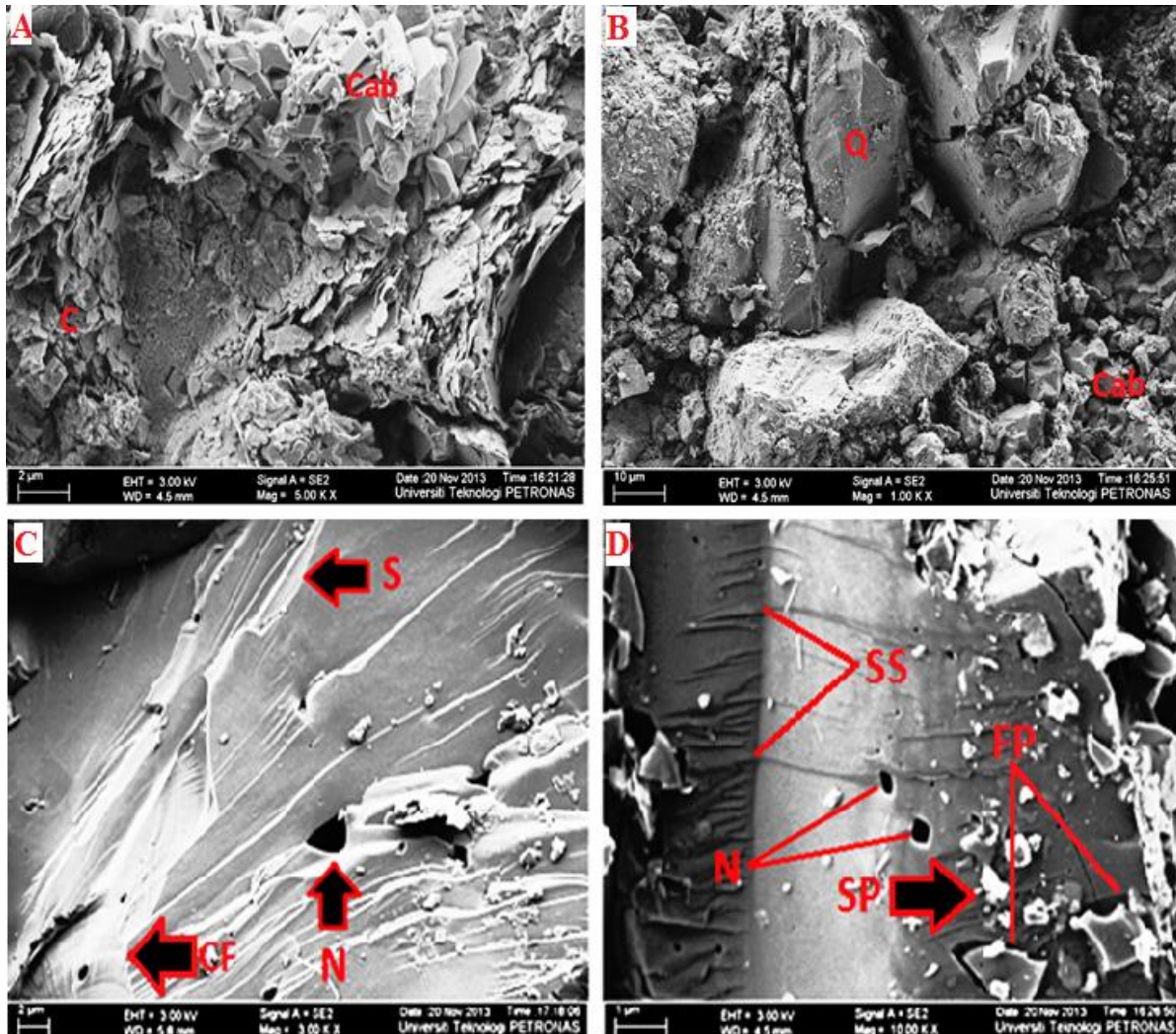


Fig. 15: The SEM micrographs showing (A) notches (N) and straight striations (SS) [F] calcite crystals (Cab) with adjacent chlorite flakes (C)

### 4.3. Porosity variation

B1 samples of Belait Formation are characterized by sutured and tangential/point grain contacts as shown in the thin section images above. The intergranular porosity ranges between 4.8 and 6%. Suturing grain contacts were also found in B2 samples, attributable to grain boundary dissolution accompanied by cementation from overburden pressure. The porosity of B2 ranged between 0.8 and 1.2%, which is relatively lower compared to the B1 samples. Conversely, B4 samples exhibited higher porosity with values between 13.6 and 13.8, while

B3 samples showed more compactness with a value range of 4.2 to 5.4%. The relatively lower porosity of B4 is possibly attributable to post depositional induration and iron oxide infiltration. The uncompact and extensively weathered Lambir rocks samples displayed higher porosity values, ranging from 9.4% in L1 to approximately 30% in L3 sample, as outlined in Table 1. These high values are consistent with the characteristic floating grain contact of the ferruginous and pyritic Lambir Formations. In contrast, the indurated calcareous (L4) sandstones show minimal porosity as low as 0.6%, evidently due to calcareous cement that invaded in situ intergranular pores.

Table 1. Porosity Values for the Facies of Belait and Lambir formations

Sample	Quartz %	Feldspar %	Other minerals [lithic fragments] %	Porosity %
B1	88.6	0	6.6	4.8
B1b	87	0	7	6
B2	70.8	0.4	28	0.8
B2b	70.6	0.2	28	1.2
B3	40.6	0	54	5.4
B3b	40.8	0	55	4.2
B4	55	0	30.4	13.8
B4b	53.6	0	32.8	13.6
L1	47.6	0	43	9.4
L1b	50.8	0	38.8	10.4
L2	37.4	0	45.4	17.2
L2b	39	0	44	17
L3	51.4	0	20.2	28.4
L3b	49.8	0	22.4	27.4
L4	46.2	0	51	2
L4B	47	0	52.4	0.6

## 5. Discussion

### 5.1. Petrographic and diagenetic variations

#### **Belait Formation**

The well consolidated quartz arenites (B1 and B2) are evidently tidal current-worked and deposited by fluvial fluid-flow process in flood tidal delta or tidal channels, as indicated by the conglomeratic constitution of the basal Belait formation. Although re-worked into the same sequence, the apparent variations in mineralogical composition between B1 and B2 point to different source materials. The presence of chlorite and plagioclase feldspar still intact in B2 indicates igneous/metamorphic origin, while the iron oxides present can be attributable to the hydration of the free  $Fe^{2+}$  generated from the dissolution of detrital chlorites (identified in FESEM images of B2) in acidic meteoric water. On the other hand, the dominant presence of compact sand sized quartz intraclasts within the framework clast of B1 indicate meta-sedimentary provenance. The morphological and microtextural features (Fig. 9) point to traction, saltation, attrition and abrasive activities associated with fluvial environment [34]. These processes reflect grain to grain impact and abrasion associated with mechanical weathering (wave action) during fluvial transportation [28]. Following deposition and continued overburden pressure, the straight and point/tangential intergranular contacts of the basal Belait siliciclastic clasts are metamorphosed to sutured, and in the case of B1, cemented by precipitated silica [30]. This is proven by the authigenic flakes of silica precipitates plastered on the detrital quartz grain, which are possibly derived from pressure induced dissolution during compaction or chemical dissolution by reactive pore fluid. Apart from point and straight grain contacts as well as suturing, mechanical compaction of B1 and B2 is further evidenced by deformational quartz twinning.

The B3 & B4 samples exhibit almost similar characteristics in terms of induration and iron oxide content. The iron oxide content are possibly derived from deeply weathered upland sediment and fed by tidal current to the shoreface sands [35]. The kaolinite and illite of B4 are possibly formed from weathering of detrital feldspar and felsic/K-rich micas in the presence of meteoric water drainage in subtropical and tropical conditions characteristic of warm and mild climate [36], which is typical of Malaysia. The relatively higher clay content, smaller sized framework grains and less fractures of B4 compared to B3 suggest comparatively farther distance of transport. However, the elongate grains and relics of suturing in B3 samples point to reworking and leaching out of matrix materials. In addition, the identified irregularly distributed v-shaped pattern, pits and fractures of B3 are microtextures that preferentially develop in medium- to high-energy subaqueous environments [30], and can also stem from several transport cycles or sediments reworking [37], all suggesting repeated fluvial action and sea transgression. Thus, the sedimentary sequence of the sampled Belait Formation area suggest sediments (B1 and B2) of high energy fluvial environment (Tidal channel) grading into shoreface deposits of B2 and B3 characterized by relatively smaller grain size, higher clay content and tangential grain contacts.

### **Lambir Formation**

In terms of provenance, the smaller grain size, and higher matrix of the Lambir sandstones evidently suggests relatively far distance of transport from source compared to the Belait rocks. The pebbly and granule content of the L1 indicate fluvial channel sedimentation. The iron oxides and organic content define the structure of the Lambir sandstones by creating laminations via rearranging the detrital grains in a preferred alignment. The alignment (laminations) of the grains with organic matter (Fig. 6B), which reduces porosity, suggest post depositional compaction from overburden pressure. The high concentration of organic matter results from the preferential deposition of fine organic matter with clay- and silt-size sandstone matrix. The presence of high iron infiltration suggests the samples are deposited in marine deltaic, nearshore and shallow offshore environments [38]. Given the insolubility of oxidized iron or  $Fe^{3+}$ , it is unlikely the iron content of B4, L1 and L2 was transported in solution from upland or sub-aerial weathering sites under oxidizing conditions of fluvial environment (rivers and streams). Therefore, the iron was presumably oxidized to insoluble  $Fe^{3+}$  under localized conditions in the shallow marine ferruginous sandstones.

However, the unstable more soluble reduced (ferrous) iron ( $Fe^{2+}$ ) indicated by the pyritic composition of L3 samples suggests water-logged soils, euxinic marine and organic-rich saline waters, all denoting anoxic environments, since oxygenated environments are particularly depleted in organic matter. The ferrous ( $Fe^{2+}$ ) ions are likely derived from local dissolution of iron-rich minerals or introduced as iron-rich fluid from an external source. The  $Fe^{2+}$  then reacts with  $H_2S$ , produced by sulfate reduction, to precipitate pyrite. The pyrite occur as clusters of globular frambroids, which can be related to the abundance of carbonaceous matter intimately mixed with the detrital iron and preserved under the strongly anoxic stratified water column which is essential for sulfide formation. The frambroids occurrence also specifies a biogenic bacterial reduction of seawater sulfate by obligate anaerobes [39]. The low permeability of the clay matrix inhibits the influx of oxygen bearing fluid into the sediments. The high concentration of pyrite and organic matter hinders silica cementation, as indicated by the friability of the rock samples. Rather, the detrital quartz grains are partially compacted / cemented by organic matter and pyrites.

The calcareous sandstones (L4) were possibly deposited in shallow water near land given the carbonate is precipitated by marine organisms that require land derived nutrients in an oxidizing environment to survive. The petrographic analysis of L4 demonstrates that the original textural relationships are retained in the calcareous sandstones, suggesting they were lithified prior to overburden deposition. The carbonate cement of the calcareous sandstones also contributes to the lithification of the sandstone. The microcrystalline calcite cement is suggested to be derived from diffusion of  $Ca^{2+}$  and  $HCO_3^-$  from overlying seawater [42]. The initial porosity becomes occupied by the infiltrated calcium rich water and mineral solutions.

The framework feldspathic or clay minerals may have been replaced with carbonate material at varying degrees ranging from grains with corroded borders to isolated residuals to complete replacement.

Although the marine samples of both formations vary from fine to coarse grained, the samples of the Belait are poorly to moderately sorted and sub-angular, while Lambir are well sorted. Thus, it can be inferred that the Lambir samples are relatively more mature due to their farther distance from source and extensive re-working, suggesting different phases of sedimentation within the same Miocene time frame.

## **5.2. Reservoir rock quality**

The petrography of the rocks defines the reservoir rock quality of the formations. The mono-quartz rock composition of the Belait conglomerate means the Formation is able to retain low stress interval, but its inherent porosity can be inhibited by grain fracturing from overburden compaction. The pore spaces become partially or completely filled with precipitated silica, quartz flakes and wollastonite sourced from pressure solution at quartz grain contacts and brecciation, or feldspar alteration in the case of B2. Moreover, the absence of Fe oxides and relatively minor amounts of clay minerals in B1 allow their transformation into more crystalline products, as Dutton and Diggs [40] showed that the content of quartz cement is susceptible to exponential increase as the matrix content of sandstones decreases. In addition, the serrated interfaces of adjacent quartz grains promote dissolution, whereas, thermodynamically, a smooth boundary would be less advantageous. The exposed and uncoated grain surface provides space for potential nucleation sites that promote the growth of quartz cement which subsequently limits compaction. The quartz cementation can subsequently reduce porosity, but preserve permeability. The suturing, tangential and concavo-convex rock contact between the adjacent grains due to compaction and later cementation by dissolved silica allows for lithification into conglomerates and loss of initial porosity. This deduction is confirmed by the porosity values outlined in Table 1.

For the Lambir sandstones, the authigenic clays effectively preserves the porosity by completely inhibiting quartz cementation after forming layers around detrital the detrital quartz grains. The presence of the carbonate intraclasts, pyrite frambroids and iron oxides reduces thermally-activated quartz cement growth [41], while the authigenic quartz overgrowth and clay coatings act as pore lining minerals at the interstices between the grains. The clay minerals and adhering particles exhibit no apparent alignment relative to the framework grain surfaces, but partially replace detrital grains or fill voids (notches and pits) left by dissolution, and preserve the textures of the host quartz grains they replace. The direct relationship between the degree of cementation and sandstone porosity at surface conditions suggests that grain coating restricts or hinders cementation and preserves porosity during deep burial and high temperatures, but decrease permeability at pore throats. Therefore, grain coating is a determining factor for the porosity preservation potential of a formation, as well as the stability of the grain. The quartz surface deterioration and associated textural defects indicate low chemical stability. The images of Lambir sandstone indicate the dissolution and pseudomorphic replacement of silica by clay minerals and/or Fe oxides. Grain coating of the quartz by secondary minerals reduces mechanical compaction and the impact of grain to grain abrasion. The clayey and calcareous sandstones are expected to have poor depositional reservoir quality owing to their high clay matrix content, and/or ubiquitous cementation by microcrystalline calcite. The calcite-cement is likely to serve as fluid-flow hindering blocks during diagenesis and hydrocarbon production. Nonetheless, the features observed on the exposed quartz surface such as etch pits and notches will promote the further dissolution of the quartz mineral. Moreover, the friable to poorly lithified sandstone beds would expectedly evolve into excellent reservoir beds, as evidenced by the high and well interconnected intergranular pores spaces and the dominant point floating grain contacts between the framework grains.

## 6. Conclusion

The petrographic and microtextural observations have differentiated a suite of facies associations which combined record a complex sequence of coastal processes in a shoreface-delta front to embayed coastal setting. The alternations or variability are considered to be the results of fluctuating rates of detrital deposition and climate effect, with the calcareous sandstone representing temporally and spatially restricted locales characterized by little or no deposition, and the sandstone beds representing contiguous areas of more rapid detrital deposition. It can be deduced that provenance significantly influences reservoir quality by controlling the composition of sediments, which in turn impacts on mechanical properties and chemical processes that decrease or preserve porosity and permeability. Despite the fact that the iron oxides serve as coating materials, they preserve the textures of the detrital quartz grains and also inhibit or delay cementation, consequently preserving porosity and permeability. The presence of the carbonate intraclasts, pyrite frambroids and iron oxides in the Lambir sandstones reduces thermally-activated quartz cement growth, although they plug intergranular pore spaces. In all, the Marine Miocene Lambir Formation represents tentative reservoir units correlatable to the prolific, hydrocarbon-bearing Baram Delta Province, and thus should be further explored.

## References

- [1] Tan, DNK, Abdul Hadi. Abd. Rahman, Azlina Anuar, Boniface Bait & Chow Kok Tho. 1999. West Baram Delta. *The Petroleum Geology and Resources of Malaysia*, Petroliaam Nasional Berhad (Petronas), Kuala Lumpur, pp. 293-341.
- [2] PETRONAS, 2013, Petronas Announces Oil and Gas Discovery Onshore Sarawak, Petronas Media Release (2013, January 18) Retrieved from <http://www.petronas.com.my/media-relations/media-releases/Pages/article/PETRONAS-ANNOUNCES-OIL-AND-GAS-Discovery-ONSHORE-SARAWAK.aspx>.
- [3] Liechti P, Roe FW, Haile NS. 1960. The geology of Sarawak, Brunei and western part of north Borneo. *Borneo: Bulletin of Brit. Borneo Geology Survey*.
- [5] Anuar A, Hoesni, MJ. 2008, The hydrocarbon property variation in the West Baram Delta petroleum system: unravelling the respective effects of biodegradation and source facies, AAPG International Conference and Exhibition, Cape Town, South Africa. October 22 (2008).
- [6] Rijks, E.J.H. 1981. Baram delta geology and hydrocarbon occurrence, *Geo. Surv. Malays. Bull.*, 14 (1981), pp. 1–18.
- [7] Togunwa OS, Abdullah WH, Hakimi MH, Barbeito PJ. 2015. Organic geochemical and petrographic characteristics of Neogene organic-rich sediments from the onshore West Baram Delta Province, Sarawak Basin: Implications for source rocks and hydrocarbon generation potential, *Marine and Petroleum Geology*, Volume 63: 115–126.
- [8] Amir, M.H., Johnson, H.D., Allison, P.A., & Hasiah W. 2013. Journal of Asian Earth Sciences Sedimentology and stratigraphic development of the upper Nyalau Formation ( Early Miocene ), Sarawak , Malaysia : A mixed wave- and tide-influenced coastal system. *Journal of Asian Earth Sciences*, 76, 301–311.
- [9] Cullen A. 2014. Nature and significance of the West Baram and Tinjar Lines, NW Borneo. *Marine and Petroleum Geology*, 51, 197–209.
- [10] Hall R. 2002. Cenozoic geological and plate tectonic evolution of SE Asia and the SW Pacific: computer-based reconstructions, model and animations, *Journal of Asian earth sciences* 20: 353-431.
- [11] Hiscott R.N. 2001. Depositional sequence controlled by high rates of sediment supply, sea level variations, and growth faulting: the Quaternary Baram delta of northwestern Borneo., *Marine Geology* 175: 67 – 102.

- [12] Lambaise J, J, Abdul Aziz bin Abdul Rahim, Peng CY. 2001. Facies distribution and sedimentary processes on the modern Baram Delta: implications for the reservoir sandstones of NW Borneo, *Marine and Petroleum Geology*, 19: 96 – 78.
- [13] Madon M, Cheng K, & Wong R. 2013. Journal of Asian Earth Sciences The structure and stratigraphy of deepwater Sarawak , Malaysia: Implications for tectonic evolution. *Journal of Asian Earth Sciences*, 76, 312–333.
- [14] Nagarajan R, Roy PD, Jonathan MP, Lozano R, Kessler FL, & Prasanna MV. 2014. Geochemistry of Neogene sedimentary rocks from Borneo Basin, East Malaysia: Paleo-weathering, provenance and tectonic setting. *Chemie der Erde - Geochemistry*, 74(1), 139–146.
- [15] Kassab MA, Hassanain IM, Salem AM. 2014. Petrography, diagenesis and reservoir characteristics of the Pre-Cenomanian sandstone, Sheikh Attia area, East Central Sinai, Egypt, *Journal of African Earth Sciences*, 96: 122 – 138.
- [16] Kord, M, Turner B, Salem AM. 2011. Linking diagenesis to sequence stratigraphy in fluvial and shallow marine sandstones: Evidence from the Cambrian–Ordovician lower sandstone unit in southwestern Sinai, Egypt, *Marine and Petroleum Geology*, 28: 1554 – 1571.
- [17] Salem AM, Abdel-Wahab, A, McBride EF. 1998. Diagenesis of shallowly buried cratonic sandstones, southwest Sinai, Egypt. *Sedimentary Geology*. 110: 311 – 335.
- [18] Holloway NH. 1982. North Palawan block, Philippines—Its relation to Asian mainland and role in evolution of South China Sea. *American Association of Petroleum Geologists Bulletin* 66, 1355–1383.
- [19] Hutchison CS. 2005. *Geology of North-West Borneo: Sarawak, Brunei and Sabah*. Elsevier, Amsterdam, 421 pp.
- [20] Madon M. 1999. Basin types, tectono-stratigraphic provinces, and structural styles. In: *The Petroleum Geology and Resources of Malaysia*. PETRONAS, Kuala Lumpur, pp. 77–112.
- [21] Tan DNK, Lamy JM. 1990. Tectonic evolution of the NW Sabah continental margin since the Late Eocene. *Bulletin of the Geological Society of Malaysia* 27, 241–260.
- [22] Haile NS. 1968. Geosynclinal theory and the organizational pattern of the Northwest Borneo Geosyncline. *Quarterly Journal of the Geological Society* 124, 171–188.
- [23] Norzita MF, Lambiase JL. 2014. Ichnology of shallow marine clastic facies in the Belait Formation, Brunei Darussalam. *Bulletin of the Geological Society of Malaysia*, Volume 60, December, pp. 55 – 63.
- [24] Wilford GE. 1961. The geology and mineral resources of Brunei and adjacent parts of Sarawak. *Borneo: Geological Survey British Territory in Borneo*.
- [25] Ali A, Padmanabhan E. 2013. Quartz surface morphology of Tertiary rocks from North East Sarawak, Malaysia: Implications for paleo-depositional environment and reservoir rock quality predictions. *Petroleum exploration and development* 41, 6.
- [26] Geological Society of Malaysia. 1995. *Annual report of the geological society of Malaysia, 1995*. Kuala Lumpur, Malaysia: Geological Survey Department, Ministry of Primary Industries.
- [27] Nagarajan R, Armstrong-Altrin JS, Kessler FL, Hidalgo-Moral EL, Dodge-Wan D, and Nur Iskandar Taib. 2015, Provenance and tectonic setting of Miocene siliciclastic sediments, Sibuti formation, northwestern Borneo. *Arabian Journal of Geosciences*, 8(10), 8549-8565.
- [28] Armstrong-Altrin JS, Madhavaraju J, Ramasamy S, et al. 2005. Provenance and depositional history of sandstones from the Upper Miocene Kudankulam Formation, Tamil Nadu. *Journal of Geology Society in India*, 66: 59–65.
- [29] Alekseeva VA, Hounslow MW. 2004. Clastic sediment source characterization using discrete and included magnetic particles—their relationship to conventional petrographic methods in early Pleistocene fluvial-glacial sediments, Upper Don River Basin (Russia). *Phys Chem Earth* 29:961–971.

- [30] Krinsley DHA, Dornkamp JC. 1973. Atlas of quartz sand surface textures. New York: Cambridge University Press.
- [31] Chakroun A, Miskovsky JC, Zaghib-Turki D. 2009. Quartz grain surface features in environmental determination of aeolian Quaternary deposits in northeastern Tunisia. *Mineral Mag* 73(4):607–614.
- [32] Peterknecht KM, Tietz G F. 2011. Chattermark trails: surface features on detrital quartz grains indicative of a tropical climate. *J Sediment Res* 81:153–158.
- [34] Madhavaraju J, Carlos J, Hussain SM, & Mohan SP. 2009. Microtextures on quartz grains in the beach sediments of Puerto Peñasco and Bahia Kino, Gulf of California, Sonora , Mexico, 367–379.
- [35] Van Houten FB., 2000. Ooidal ironstones and phosphorites – A comparison from a stratigrapher’s view, in Glen, C.R., L. Prevot-Lucas, and J. Lucas (eds), *Marine Authigenesis: From global to Microbial*: SEPM Special Publication 66, pp. 127-132.
- [36] Bjørlykke K. 1998. Clay mineral diagenesis in sedimentary basins - a key to the prediction of rock properties; examples from the North Sea Basin. *Clay Minerals* 33(1): 15-34.
- [37] Corcoran PL, Packer K, Biesinger MC. 2010. First cycle grain weathering processes: Compositions and textures of sea glass from port allen, Kauai, Hawaii. *Journal of Sedimentary Research*, 80: 884–894.
- [38] Petranek J. and Van Houten FB. 1997. Phanerozoic Ooidal Ironstones: Czech Geological Survey Special Paper 7.
- [39] Berner RA. 1982. Burial of organic carbon and pyrite sulfur in the modern ocean: its geochemical and environmental significance. *Am. J. Sci.*, 282, 451 – 473.
- [40] Dutton SP and Diggs TN. 1990, History of quartz cementation in the Lower Cretaceous Travis Peak Formation, east Texas: *J. Sediment. Petrol.*, 60, 191-192.
- [41] Deane SM. 2010. Quartz grain microtextures and sediment provenance: Using scanning electron microscopy to characterize tropical highland sediments from Costa Rica and the Dominican Republic [D]. Knoxville: University of Tennessee, Knoxville: 123.
- [42] Al-Ramadan K. 2006. Impact of Diagenetic Alterations on Reservoir Quality and Heterogeneity of Paralic and Shallow Marine Sandstones. Links to Depositional Facies and Sequence Stratigraphy Acta Universitatis Upsaliensis Uppsala. *Digital Comprehensive Summaries of Uppsala Dissertations from the Faculty of Science and Technology* 195. 57 pp. Uppsala ISBN 91-554-6588-9.
- [43] Armstrong-Altrin JS, Natalhy-Pineda O. 2013. Microtextures of detrital sand grains from the Tecolutla, Nautla, and Veracruz beaches, western Gulf of Mexico, Mexico: implications for depositional environment and paleoclimate. *Arab Journal of geosciences*. DOI 10.1007/s12517-013-1088-x.
- [44] Boggs, Jr S. *Petrology of Sedimentary Rocks*. Cambridge University Press; 2009. P. 506 – 508.

---

\* Corresponding author: [alicorp07@gmail.com](mailto:alicorp07@gmail.com); +60169165850